

Conference Paper

Experimental Studies of the Initial Section in the Channel Simulator of a Heat-Releasing Element Cell

E.F. Avdeev, V.O. Smirnova, and Tran Hong Phuc

Obninsk Institute for Nuclear Power Engineering of the National Research Nuclear University MEPhI, Studgorodok 1, Obninsk, Kaluga region, 249040, Russia

The study had provided complete measurement results of the velocity field and the pressure loss of the initial section in the channel of the scaled-up close-packed model of the heat-releasing element cell. It also provides estimates of pressure losses based on the boundary layer calculation and their comparison with the experimental ones.

In the study of the initial sections, even circular tubes, only a few scientific works have been conducted. The most complete and comprehensive of them were performed by Trubakov Yu.P. (SSC-RF-IPPE) assigned by academician Subbotin V.I.

The experiments were carried out by the authors of this work on a close-packed model of the heat-releasing element cell with the relative lattice spacing $\frac{S}{d_{HR}} = 1,014$.

The initial section of the tube has velocity field deformation along the length. With a soft start of the real liquid into a tube of any vessel, we will have an almost even velocity distribution. Further, a boundary layer appears on the walls of the tube, and in the central part one can observe an inviscid (external in relation to the boundary layer) flow, surrounded by a boundary layer (Fig. 1).

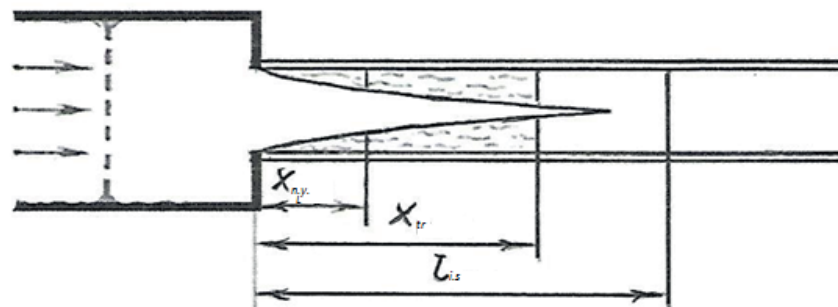


Figure 1: Formation of the initial section in channels.

The velocity profile, which is uniform in the initial section, deforms with with the increase of $\frac{x}{d}$ (Figure 2a). Meanwhile, the thickness of the boundary layer increases, and the nuclear cross section (sector with a uniform velocity profile) is decreasing.

OPEN ACCESS

Corresponding Author:
 V. O. Smirnova
 konstansta@yandex.ru

Received: 23 December 2017
 Accepted: 15 January 2018
 Published: 21 February 2018

Publishing services provided by
 Knowledge E

© E.F. Avdeev et al. This article is distributed under the terms of the [Creative Commons Attribution License](#), which permits unrestricted use and redistribution provided that the original author and source are credited.

Selection and Peer-review under the responsibility of the AtomFuture Conference Committee.

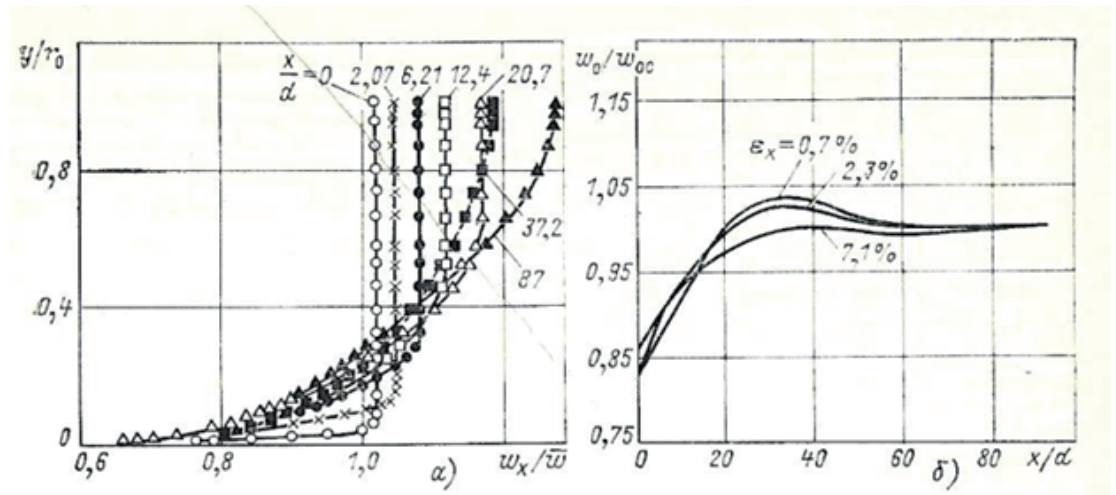


Figure 2: The velocity profiles in the initial section of the tube at different distances from the input x / d at $Re = 4.5 \times 10^3$ (a) and the velocity change at the axis along the length of the initial section for different ϵ_x (b) values.

Simultaneously, the flow in the boundary layer is inhibited, and in the core, by the condition of continuity, accelerates. Consequently, transverse velocity components directed from the wall to the axis, that enable the flow of fluid from the boundary layer to the core of the flow, are present in the flow. At $\frac{x}{d_g} \approx 40$ the velocity profile becomes most elongated (i.e., the least full), the velocity on the axis reaches the peak value. In this section, the core of the flow disappears, but the stabilization of the flow is not yet attained. With further increase of $\frac{x}{d_g}$ the filling of the velocity profile again increases, the velocity on the axis decreases and at a distance from the input, which is equal to the length of the hydrodynamic initial section ($x = l_{h,r}$), the flow becomes stabilized, that is, with the subsequent increase in x / d , the velocity profile remains unchanged. Thus, the velocity at the axis of the tube (V_0) first grows, goes through a maximum point, and then slowly decreases, tending to a constant value (V_{0c}) (Figure 2b) [2].

The understanding that the pressure losses at the initial section can not be calculated by known formulas for a stabilized turbulent flow is related to the understanding of the velocity field deformation in these sections. With a large elongation of the heat-releasing element ($\frac{x}{d_g} > 350$) an error in pressure losses determination will be negligible. However, for small-sized active zones the error can be up to 50%. And this is especially important in carrying out experiments on scaled-up models, when determining the heat transfer coefficients. The tasks for the experiment were as follows:

1. Calibration of the metering orifice to determine the average velocity in the channel of the cell;

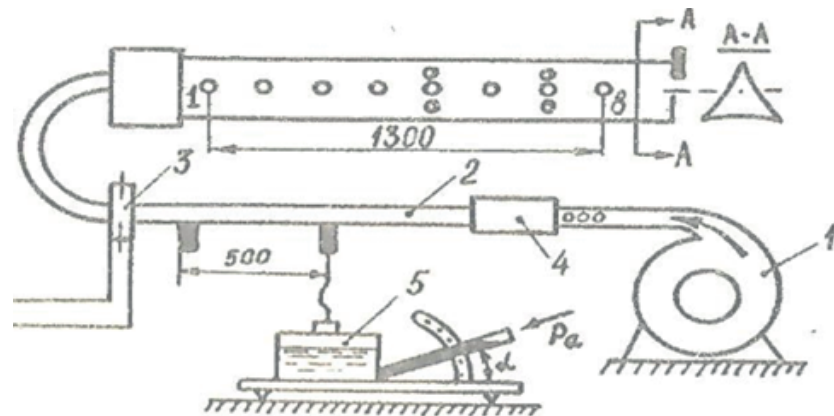


Figure 3: The scheme of the experimental stand. 1) blast engine; 2) circular tube; 3) measuring orifice; 4) test area; 5) micromanometer.

2. Establishment of flow regimes and hydraulic smoothness or roughness of the channel walls;
3. Measurement of velocity distribution in channel sections;
4. Determination of the velocity change on the axis of the initial section;
5. Estimation of the initial section length;
6. Measurement of pressure losses in the initial section and comparison with the calculated data for the stabilized flow;
7. Evaluation of the pressure losses based on an approximate calculation of the boundary layer.

Metrological support of measurements was carried out by microtubes made in the workshops of the hydroaerodynamics department, in the 1960s, at the Leningrad Polytechnic Institute.

The stand is serviced by the staff of the Department of Thermal Physics of the INPE. The stand includes a channel simulating the channel of the heat-releasing cell.

Pitot tube, a microtubule and micromanometers were used as the primary sensors for measuring pressures.

The scheme of the experimental stand is shown in Fig. 3.

Fig. 4 shows the general view of the experimental stand.

Before entering the test channel, the stand has a section with stabilized flow in a circular tube. The flow rate in the circular tube will be the same as in the test channel by the condition of maintaining the mass flow.

TABLE 1: Characteristics of the experimental stand.

General characteristics of the heat-releasing channel simulator	
Total length of the main circuit	~ 1,5 m
Length of the test section from input to point 1	~ 0,2 m
Length of the test section from input to point 2	0,35 m
Length of the test section from input to point 3	0,5m
Length of the test section from input to point 4	0,65m
Length of the test section from input to point 5	0,85m
Length of the test section from input to point 6	1,1m
Length of the test section from input to point 7	1,35m
Length of the test section from input to point 8	1,45m
Length of the test section from input to the output	1,5m
Hydraulic diameter of the triangular channel	23,95mm
Wetted perimeter of the triangular channel	180mm
Sectional area of the triangular channel	1078mm ²
Diameter of heat-releasing cell	137,35mm
Step between heat-releasing cells	2mm
Inside tube diameter	26,5mm
Length at which the pressure drop across the circular tube was measured	500mm
Thickness of the triangular channel walls	4mm
Relative grid pitch	1,014

The flow rate in the circular tube was determined by the well-known formula for turbulent flow in circular tubes, developed and patented at the Department of Thermal Physics of the National Research Nuclear University MEPhI [3]:

$$Q = \pi a^2 \left(U_{\max} - 2,885 \sqrt{\frac{\Delta p a}{L \rho}} \right) \quad (1)$$

Where a - internal radius of tube;

u_{\max} - maximum velocity on the axis of the tube;

Δp - the pressure drop across the length L ;

ρ - ambient density.



Figure 4: General view of the experimental stand.

The average velocity in the test channel is based on the pressure drop on the orifice, which was previously tared using formula (1):

$$V_{\text{avg}} = 0,2487 \sqrt{\frac{\Delta p_{\text{dip}}}{\rho}} \quad (2)$$

The hydraulic channel junction was determined traditionally: from the measured pressure drops and the average velocity in the channel and the subsequent construction of the dependence $\log \Delta P \sim \log V_{\text{avg}}$.

According to the calculated coefficient of frictional resistance on the stabilized section of the test channel was the height of the hillock of sand roughness in the approximation of a circular tube with a diameter equal to the hydraulic diameter of the heat-releasing cell.

$$k_s = \frac{a}{10^{\left(\frac{1}{2\sqrt{\lambda_{\text{exp}}}} - 0,87\right)}} = \frac{11,975}{10^{\left(\frac{1}{2\sqrt{0,0414}} - 0,87\right)}} = 0,3098\text{mm}$$

The value of the hillock is 0.31 mm, and the thickness of the laminar sublayer $\delta=0,27$ MM.

The measurement of the velocity distribution in the cross sections of the channel was carried out by microtubes (Figure 5), with measurements of the difference between the braking pressure and static pressure. On the channel there are 8 holes through which the microtubes were successively injected. The measurement of velocities began at a distance of 0.6 mm from the wall.



Figure 5: Microtubule.

The experimental data of velocity were determined from the condition of the adiabatic process in the gas:

$$V_1 = \sqrt{\frac{2k\Delta p_0}{(k-1)\rho_0} \left[1 - \left(\frac{p_1}{p_0} \right)^{\frac{k-1}{k}} \right]} \quad (3)$$

Where: k – ratio of heat capacity at constant pressure and volume;

P_0 – stagnation pressure (Pa);

P_1 – static pressure (Pa), determined from the pressure P_0 ;

ρ_0 – is the density of air.

Examples of the velocity distribution are shown in Fig. 6.

Where the length of the test area from the input to point 1 is ~ 0.2 m;

To point 2 - 0.35 m;

To point 3 - 0,5 m;

To point 4 - 0,65 m;

To point 6 - 1,1 m;

To point 9 (channel output) - 1.5m.

In the course of the experiment, the velocity distribution was measured at 3 different rates corresponding to pressure drops on the orifice 1.4 KPa, 1.6 KPa, 1.7 KPa. Based on this, a graph of the dependence has been constructed $\frac{V_{\max}}{V_{\text{avg}}} \sim \frac{x}{d_g}$ (Рис. 7).

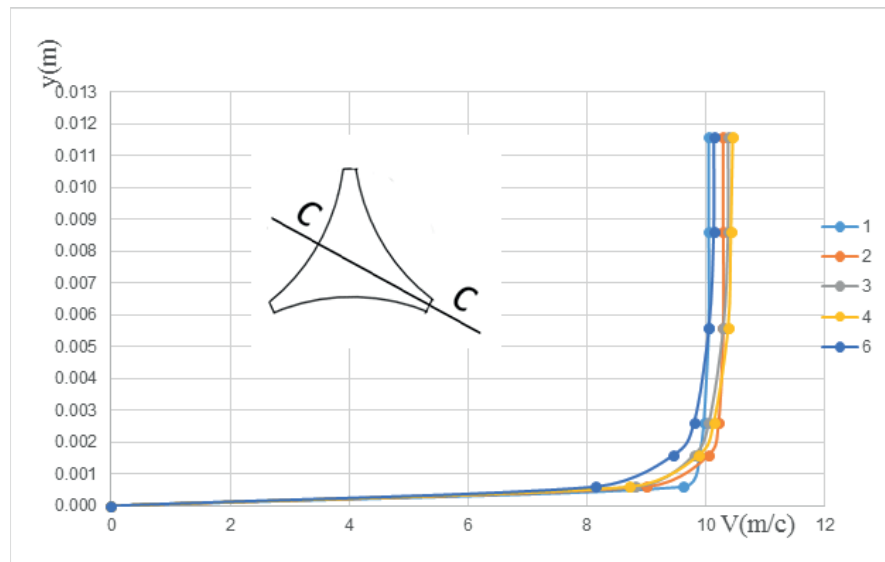


Figure 6: Distribution of velocities in the cross sections of the channel in the direction CC.

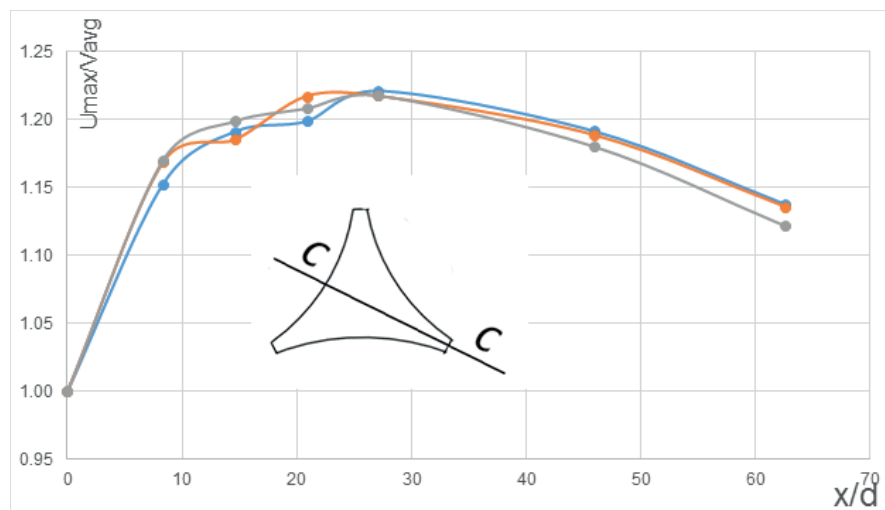


Figure 7: Change of the maximum velocity along the initial section.

From the graph it follows that the maximum velocity first increases, then decreases and remains constant until the output of the channel. In comparison with the maximum velocity, the average increase is 22%.

The length of the initial section was determined from the graph. The maximum velocity is at point 4 at $x = 65$ sm. $\frac{x}{d_g} = 36,5$.

The length of the initial section of the heat-releasing cell channel was 36.5 gauges, which is smaller than the length of the initial section in circular tubes ($\frac{x}{d_g} \approx 50$).

The measured pressure losses in the initial section for one of the regimes on the heat-releasing cell channel simulator were $\Delta p = 63.7$ Pa. According to calculations for a stabilized flow, $\Delta p = 36.67$ Pa, which is 42.5% less than the actual pressure loss.

Calculation of pressure losses for the stabilized flow was carried out using the formula for the friction coefficient of the tight packing of heat-releasing elements ($x/d < 1.02$) [4].

In addition, the estimated pressure losses are based on an approximate calculation of the turbulent boundary layer on a hydraulically damped plate using the T. Karman integral relation (according to V.F. Droblenkov) [1].

$$\frac{d\delta^{**}}{dx} + \frac{U'\delta^{**}}{U} \left(2 + \frac{\delta^*}{\delta^{**}} \right) = \frac{\tau_w}{\rho U^2} \quad (4)$$

Where $\delta^* = \int_0^\delta (1 - \frac{u}{U}) dy$ – displacement thickness;

$\delta^{**} = \int_0^\delta (1 - \frac{u}{U}) \frac{u}{U} dy$ – momentum thickness;

U – boundary-layer velocity;

$U' = \frac{dU}{dx}$ – velocity change along the boundary-layer;

τ_w - wall frictional stress.

Formula (4) takes into account the lateral pressure gradient $\frac{dP}{dx}$:

$$P + \frac{\rho U^2}{2} = const, \quad \frac{dP}{dx} = 2U\rho \frac{dU}{dx};$$

In other words, the factor in front of the bracket takes into account the lateral change in pressure.

When calculating the initial section, the velocity at the boundary layer coincides with the velocity along the axis of the initial section, which increases.

The method was generalized for the case of a rough platinum by VF Droblenkov, when $\frac{\tau_w}{\rho U^2}$ does not depend on the Reynolds number, but only on the local relative coarseness δ^{**}/k .

The width of the plate was assumed to be equal to the perimeter of the heat-releasing cell. At the same time it turned out that in order the calculations match, the empirical Droblenkov coefficient must be increased approximately 1.3 times and assumed equal to $4,03 \cdot 10^{-3}$. For the frictional stress, the Droblenkov formula in the form could be used:

$$\frac{\tau_w}{\rho U^2} = 4,03 \cdot 10^{-3} \left(\frac{\delta^{**}}{k} \right)^{-\frac{1}{6}} \quad (5)$$

The frictional resistance along the length of platinum L was determined by integration through the friction coefficient C_{f0} :

$$C_{f0} = \frac{\int_0^L \tau_w dx}{\frac{1}{2} \rho U^2} = 0,0162 \left(\frac{L}{k} \right)^{-1/7} \quad (6)$$

The pressure losses at individual sections were calculated with the formula:

$$\Delta p_i = \frac{\tau_i \chi L_i}{\sigma_{cel.}}$$

Where τ_i – frictional stress; $\sigma_{cel.}$ – cross-sectional area of fuel cell; $i = 1,2,3,4,5$.

The calculation of the pressure loss across the entire initial section is measured with totalization of Δp_i in certain areas.

Under the condition of the experimental and calculated values of pressure losses coincidence, a change in the empirical Droblenkov coefficient from 0.0031 to 0.00403 was found.

1. Conclusion

1. The length of the initial section in the channel of the heat-releasing cell, found from the measured velocity field, turned out to be much shorter than in the circular tube.
2. It is shown that the pressure losses at the initial section can not be calculated from the formulas for the stabilized flow. According to the results of the performed experiments, the decrease in pressure loss makes up 42.5%.
3. The frictional stress values along the perimeter of the heat-releasing cell differ by more than 20%.
4. Pressure losses in the initial section can be calculated on the basis of an approximate calculation of the boundary layer on the hydraulically damped plate equal to the perimeter of the heat-releasing cell, but with a modified empirical Droblenkov coefficient.

References

- [1] Loytsiansky L. G. Mechanics of fluid and gas / logarithmic and power-law formulas for the resistance of smooth and rough pipes. Textbook. for universities. - 7 th ed., Rev. - M.: Dhofa, 2003. p. 671.
- [2] Petukhov B. S., Genin L. G., Kovalev S. A. / Edited by Petukhov B. S. heat exchange in nuclear power plants. -2-e ed.,Revis. and aug. - M: Energoatomizdat, 1986. - 472 p.
- [3] Avdeev E.F., Bolshunova V.V. Method of determining the flow in a pipe-line // Patent of Russia No. 2169905. 2001.



- [4] Avdeev E. F. Calculation of the hydraulic characteristics of the reactor circuit. The manual for the course "Thermodynamics and Thermal Physics of Nuclear Power Generation" - Obninsk, 1991-62p.